Design of a New Wideband Single-Layer Reflective Metasurface Unit Cell for 5G-Communication

Muhammad A. Qureshi [1], Abdul Aziz [1], Asjad Amin [1], Hafiz Faiz Rasool [2*], and Faisal Hayat [3]

[1] Department of Telecommunication Engineering, The Islamia University of Bahawalpur, 63100, Pakistan
ali.qureshi@iub.edu.pk, abdul.aziz@iub.edu.pk, asjad.amin@iub.edu.pk

[2] School of Information and Electronics, Beijing Institute of Technology, Beijing, China
hafiz@bit.edu.cn*

[3] Department of Computer Engineering, University of Engineering and Technology, Lahore, Pakistan
faisal.hayat@kics.edu.pk

Abstract **—** In this paper, a new single layer subwavelength unit cell is designed for reflective metasurface at 28 GHz suitable for 5G communication with linear phase response and wide bandwidth characteristics. The proposed unit cell is analyzed through Floquet mode analysis for two different sizes. The unit cell with conventional half-wavelength size (HWS) has achieved $590°$ phase range while the unit cell with a subwavelength size (SWS) of $\lambda/3$ has achieved exactly $360°$phase range. It is observed that the unit cell with SWS provides linear phase response as compared to the unit cell with HWS. Since non-linear phase response may produce more phase errors on wide range of frequencies, so SWS unit cell with $360°$ phase range and linear phase response is more suitable option for wideband operation as compared to conventional HWS unit cell with more than $360°$ phase range.

Index Terms **—** 5G communication, metasurface, reflectarray, reflective, subwavelength, wideband.

I. INTRODUCTION

Antenna array beamforming has a key role to achieve higher data rates in 5G communication system [1,2]. Reflective metasurface (RM) or reflectarray antennas are widely used to generate high directional pencil beams and considered as the most promising solution for point to point and 5G communication systems [3-6]. RM is a low-cost and low-profile solution as compared to the conventional parabolic reflectors. Despite its various advantages, RM has narrow bandwidth due to inherent narrow-band nature of microstrip elements and phase dispersion due to non-linear phase response of such elements.

An RM unit cell needs to achieve at least $360°$ phase shift range for compensation of phase delays [7]. This phase shift range is usually achieved by varying the size of the patch element within the fixed size of the unit cell. A conventional unit cell size is usually half-wavelength at designed frequency to avoid grating lobes [7]. However, the phase curve achieved by such unit cell size is usually non-linear that results in significant phase errors particularly when frequency is different from the designed frequency [8]. Due to such significant phase errors the metasurface cannot be used for wideband operation. However, if phase response is linear then such phase errors will be reduced significantly due to less sensitivity of phase curve.

During the past few years, various wideband approaches have been proposed to improve bandwidth performance for RM. Multi-resonant element [9-11] and subwavelength element [12-17] are famous techniques, which are usually designed with multilayer configurations with air-gap to enhance bandwidth. However, RM with multi-layer elements leads to more fabrication complexity with higher cost. In the proposed technique a single layer simple element is designed without any air-gap by combining multi-resonant element and subwavelength element techniques to achieve linear phase response and hence wideband operation for 5G communication.

To achieve the goal, first a single layer unit cell with conventional half-wavelength size (HWS) is designed that achieves $590°$ phase range with non-linear phase response at 28 GHz. The size of the unit cell is then restricted to sub-wavelength size (SWS) that achieves sufficient $360°$ phase range with linear phase response at 28 GHz for 5G communication system.

As, SWS unit cell achieved $360°$ phase range that is sufficient for phase compensation, so redundant phase range can be avoided to achieve linear phase response and hence wideband performance. SWS unit cell is also compared with HWS unit cell through sensitivity response at designed frequency and phase response over a wide range of frequencies to verify its wideband performance.

The rest of the paper is as follows. In Section II, the structure of the proposed unit cell for RM is briefly discussed. Section III discusses the performance analysis of the unit cell and finally the paper is concluded in Section IV.

II. PROPOSED UNIT CELL FOR RM

RM antenna design is mainly depending on the unit cell. The first step in the design of RM is to choose a unit cell that can span a 360° reflection phase range. By achieving this condition, we can compensate for the total phase delay from the feed to all RM elements on aperture plane in order to transform a spherical wavefront to a plane wave.

A. Unit cell structure

The unit cell for RM operates around 28 GHz for 5G communication system. The unit cell is a part of a square lattice in which proposed multi-resonant microstrip element printed on a substrate layer without air gap is shown in Fig. 1.

The proposed microstrip element of the unit cell is simple and cost effective without any fabrication complexity. The substrate used is Rogers RT/duroid 5880 with dielectric permittivity $\varepsilon r = 2.55$, thickness $h_s = 1.575$ mm, loss tangent $\delta = 0.0009$. Diameter D_o is the main parameter of the microstrip element, which is varied to control phase response. Other geometrical parameters, which are optimized through parametric analysis for the proposed microstrip element are following: $W_o = 0.3$ mm, $g_1 = 0.3$mm, $W_g = 0.3$ mm, $L_c = 0.5$ mm.

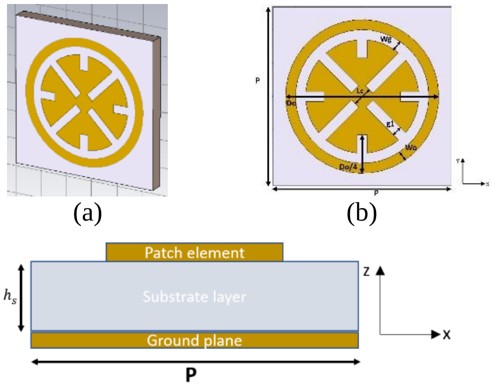

(a) (b)

(c)

Fig. 1. Configuration of the unit cell element in the proposed RM: (a) unit cell, (b) front view, and (c) side view.

B. Simulation setup and phase response

Floquet mode of CST Microwave studio suite is used to analyze the scattering characteristics of the unit cell. We use periodic boundary conditions along *x* and *y* axes whereas boundary condition for z-axis is kept open. Surface roughness of the unit cell is ignored during simulation due to availability of smooth lithographic printing facility for microstrip elements. The phase response of unit cell is analyzed for two sizes, i.e., conventional HWS with $P = 5.35$ mm (λ/2 at 28 GHz), and SWS for which $P = 3.5$ mm (λ/3 at 28 GHz). The phase responses for the SWS and HWS unit cells at 28 GHz are shown in Figs. 2 (a) and 2 (b) respectively. The diameter D_o is varied from 2 to 5.3 mm and 2 to 3.5 mm with a step size of 0.01 mm for HWS and SWS unit cells at 28 GHz, respectively. The conventional HWS unit cell achieves 590° phase range, however the phase response is non-linear, due to which more phase errors will be generated when frequency deviates from 28 GHz. On the other side, the phase response of SWS unit cell is almost linear and it achieves sufficient 360° range required to compensate phase delays. For RM design, the value of D_o may not be fixed to a single value instead several different values of D_o may be used for compensation of phase delays from 0 to 360 degree. Due to linear phase response of the SWS unit cell wideband performance is expected.

C. Parametric analysis

To achieve more than 360°phase range and linear phase response, optimum parameters are selected through parametric analysis. The phase response of a unit cell depends on element size, shape, substrate thickness and dielectric permittivity. The parametric analysis for the two critical geometrical parameters of the unit cell (L_c, and W_g) are shown here in Figs. 3 and 4 for both HWS and SWS unit cells. Other geometrical parameters are not much sensitive to phase response, so the effect of their variation is not shown here for brevity.

First, L_c is varied from 0.1 mm to 0.5 mm as shown in Fig. 3, and it can be seen that non-linear phase response of HWS unit cell is more obvious and phase response of SWS unit cell remains almost linear at all values, $L_c = 0.3$ mm is selected as an optimum value because at other values the phase range is less than 360°for SWS unit cell. Thereafter, W_g is varied from 0.2 mm to 0.4 mm while other parameters are fixed. Figure 4 shows that the phase response of HWS unit cell is still non-linear with more than 360° phase range for all values of W_g. While, the phase response for SWS unit cell becomes more linear as W_g increases, however $W_g = 0.3$ mm is selected as optimum value because it achieves exactly 360° phase range.

III. PERFORMANCE ANALYSIS

The performance of the proposed unit cell is evaluated using sensitivity, bandwidth and cross-polarization analysis.

A. Sensitivity analysis

The sensitivity of the unit cell is determined by computing the partial derivative of the reflection phase response with respect to microstrip patch size (D_o). The sensitivity analysis helps in determining the tolerance against the fabrication errors and related to the slope of the reflection phase curve, i.e., the smooth reflection phase curves exhibit more stable bandwidth performance as well as lower fabrication sensitivity or high tolerance over a wide range of frequencies with less fabrication and phase errors. Figure 5 shows the sensitive responses of the SWS and HWS unit cells. From the plots, it is observed that the SWS unit cell is less sensitive to fabrication and phase errors as compared to the HWS unit cell.

B. Bandwidth analysis

The bandwidth of the RM antenna is also determined from the reflection phase curves of the unit cell. The phase responses of both HWS and SWS unit cells are analyzed for different frequencies to observe the bandwidth of the unit cell. Figure 6 shows reflection phase response of the unit cell from 26 GHz to 30 GHz, it is observed that the reflection phase curves are linear and parallel to each other for the SWS unit cell as shown in Fig. 6 (a). On the other hand, the phase curves for HWS unit cell in Fig. 6 (b) are not as much parallel and linear particularly at the lower ends as compared to SWS unit cell and hence more significant phase errors are expected from HWS unit cell for wideband operation. It verifies significant superiority of SWS unit cell over HWS unit cell for wideband performance.

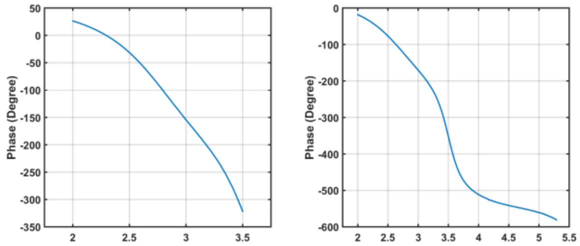

(a) (b)

Fig. 2. Phase response for the proposed: (a) SWS unit cell and (b) HWS unit cell.

C. Cross polarization analysis

The cross polarization shows isolation of a co-polarized radiation wave with an orthogonal polarized radiation wave. Since the unit cell structure is symmetric so cross polarization can be suppressed, so it is necessary to analyze cross polarization of the unit cell. The unit cell is analyzed through Floquet ports in CST Microwave Studio. For cross polarization analysis the two ports of the unit cell are used in cross polarized modes, if one port is in TE mode then the other port is converted to TM mode to see cross polarization response of the unit cell. The cross polarization of both types of unit cells is shown in Fig. 8. It is clear that the cross-polarization level is less than −40 dB in both cases. It confirms that the proposed unit cell is also suitable to achieve cross polarization isolation.

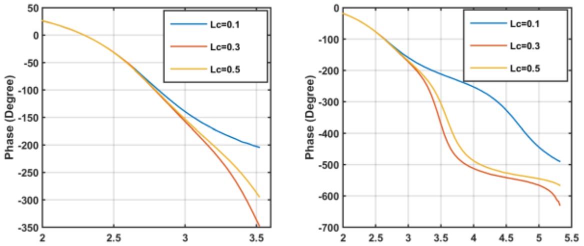

(a) (b)

Fig. 3. Phase response for the proposed unit cell for different L_c values: (a) SWS unit cell and (b) HWS unit cell.

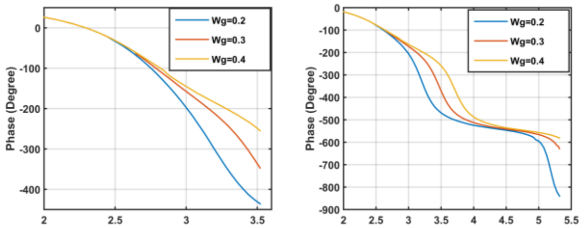

(a) (b)

Fig. 4. Phase response for the proposed unit cell for different W_g values: (a) SWS unit cell and (b) HWS unit cell.

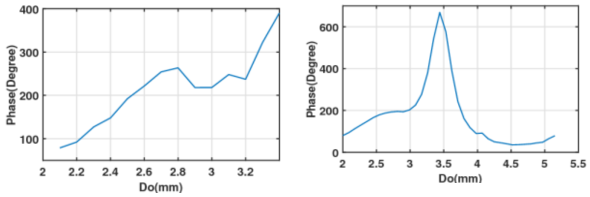

(a) (b)

Fig. 5. Sensitivity response of proposed unit cell: (a) SWS unit cell and (b) HWS unit cell.

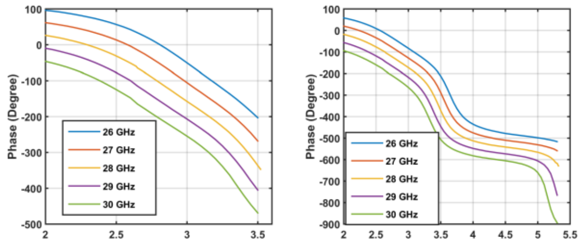

(a) (b)

Fig. 6 Bandwidth response of unit cell at 28 GHz: (a) SWS unit cell and (b) HWS unit cell.

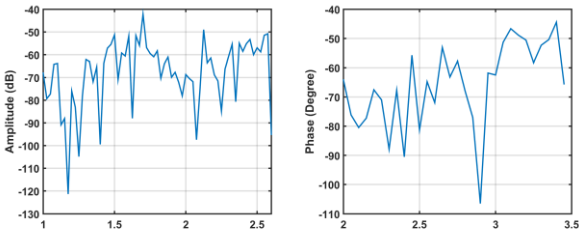

(a) (b)

Fig. 7 Cross polarization response for the proposed unit cell: (a) SWS unit cell and (b) HWS unit cell.

IV. CONCLUSION

A simple single layer RM unit cell was proposed to achieve wideband performance. The unit cell was analyzed for both HWS and SWS for a wide range of frequencies. HWS unit cell achieves 590° phase range (Fig. 2b) with non-linear phase response which is not suitable for wideband operation. The phase response for HWS unit cell remains almost linear for $D_o = 2$ to 3.3mm and becomes non-linear for $D_o = 3.3$ to 5.35mm. Thus, more phase errors will be generated due to non-linearity of phase curve that may reduce performance of the RM for a wide range of frequencies. While, the SWS unit cell provided exactly 360° phase range with almost linear phase response for $D_o = 2$ to 3.5 mm (Fig. 2 (a)). Moreover, the phase response curves remain almost linear and parallel for a wide range of frequencies (Fig. 6 (a)), which complements the wide bandwidth requirement of RM for 5G communication systems. Sensitivity (Fig. 5) and cross polarization analysis (Fig. 7) of the unit cell also demonstrated that SWS unit cell is simple and cost effective without any fabrication complexity and it also achieves good cross polarization isolation.

REFERENCES

[1] E. Ali, M. Ismail, R. Nordin, and N. F. Abdulah, “Beamforming techniques for massive MIMO systems in 5G: Overview, classification, and trends for future research,” *Frontiers Inf. Technol. Electronic Eng*., vol. 18, no. 6, pp. 753-772, 2017.

[2] A. Aziz, M. A. Qureshi, M. J. Iqbal, S. Z. A. Zaidi, U. Farooq, and U. Ahmad, “Performance and quality analysis of adaptive beamforming algorithms (LMS, CMA, RLS & CGM) for smart antennas,” *Int. Conference on Computer and Electrical Engineering*, vol. 6, pp. 302-306, 2010.

[3] M. H. Dahri, M. H. Jamaluddin, M. I. Abbasi, and M. R. Kamarudin, “A review of wideband reflect-array antennas for 5G communication systems,” *IEEE Access*, vol. 5, pp. 17803-17815, 2017.

[4] R. R. Elsharkawy, M. Hindy, A. A. Saleeb, and E. S. M. El-Rabaie, “A reflectarray with octagonal unit cells for 5-G applications,” *Wireless Pers. Commun*., vol. 97, no. 2, pp. 2999-3016, 2017.

[5] W. Hong, Z. H. Jiang, C. Yu, J. Zhou, P. Chen, Z. Yu, H. Zhang, B. Yang, X. Pang, M. Jiang, Y. Cheng, M. Al-Nuaimi, Y. Zhang, J. Chen, and S. He, “Multibeam antenna technologies for 5G wireless communications”, *IEEE Trans. Antennas Propag*., vol. 65, no. 12, pp. 6231-6249, 2017.

[6] J. Huang and J. A. Encinar, *Reflectarray Antennas*. vol. 30, John Wiley & Sons, 2007.

[7] J. Shaker, M. R. Chaharmir, and J. Ethier, *Reflectarray Antennas: Analysis, Design, Fabrication, and Measurement*. Artech House, 2013.

[8] P. Nayeri, F. Yang, and A. Z. Elsherbeni, *Reflectarray Antennas: Theory, Designs and Applications*. John Wiley & Sons, 2018.

[9] M. Chaharmir and J. Shaker, “Broadband reflectarray with combination of cross and rectangle loop elements,” *Electron. Lett*., vol. 44, no. 11, pp. 658-659, 2008.

[10] J. A. Encinar and J. A. Zornoza, “Broadband design of three-layer printed reflectarrays,” *IEEE Trans. Antennas Propag.*, vol. 51, no. 7, pp. 1662-1664, 2003.

[11] E. C. Choi and S. Nam, “W-band low phase sensitivity reflectarray antennas with wideband characteristics considering the effect of angle of incidence,” *IEEE Access*, 2020.

[12] J. Wang, Y. Zhou, S Gao, and Q. Luo, “An efficiency-improved tightly coupled dipole reflect-array antenna using variant-coupling-capacitance method,” *IEEE Access*, vol. 8, pp. 37314-37320, 2020.

[13] P. Nayeri, F. Yang, and A. Z. Elsherbeni, “Broadband reflectarray antennas using double-layer subwavelength patch elements,” *IEEE Antennas Wirel. Propag. Lett.*, vol. 9, pp. 1139-1142, 2010.

[14] P. Nayeri, F. Yang, and A. Z. Elsherbeni, “Bandwidth improvement of reflectarray antennas using closely spaced elements,” *Prog. Electromagn. Res. C*, vol. 18, pp. 19-29, 2011.

[15] J. Wu, X. Da, B. Lin, J. Zhao, and K. Wu, “Circularly polarized low-cost wide band reflect-array antenna constructed with subwavelength elements,” *Int. J. RF Microwave Comput. Aided Eng.*, vol. 28, no. 6, pp. e21277, 2018.

[16] J. Wang, Y. Zhou, and X. Feng, “A dual-polarized wideband tightly coupled reflectarray antenna proposed for 5G communication,” *Proc. Computing, Communications & IoT Applications (ComComAp)*, IEEE, pp. 200-203, 2019.

[17] Z. Akram, X. Li, Z. Qi, A. Aziz, L. Yu, H. Zhu, X. Jiang, and X. Li, “Wideband vortex beam reflectarray design using quarter-wavelength element,” *IEEE Antennas Wirel. Propag. Lett.*, vol. 18, no. 7, pp. 1458-1462, 2019.